OPEN
Original article

Nuclear Medicine Communications

^{18}F-FDG PET/CT imaging features of patients with multicentric Castleman disease

Yuanyuan Jiang[a,b]*, Guozhu Hou[a,b]*, Zhaohui Zhu[a,b], Li Huo[a,b], Fang Li[a,b] and Wuying Cheng[a,b]

Objective **The aim of this study is to investigate the role of ^{18}F-fluorodeoxyglucose (FDG) PET/computed tomography (CT) in the evaluation of multicentric Castleman disease (MCD).**

Methods **Thirty-five patients with pathologically confirmed MCD who underwent ^{18}F-FDG PET/CT were retrospectively included. The FDG uptake and CT findings of lymph nodes, pulmonary involvement, spleen, and bone marrow were assessed and the maximum standardized uptake value (SUVmax) of each lesion was measured. The locations of lymph nodes were also evaluated.**

Results **^{18}F-FDG PET/CT showed increased uptake in multiple nodal regions in 34 out of 35 MCD patients. The most frequently involved nodal sites were the cervical, iliac, axillary, and inguinal areas, and the least common was paraaortic and abdominal nodes. The involved lymph nodes were not confluent and presented a relatively symmetric pattern on PET/CT images. The highest SUVmax of lymph nodes per patient ranged from 2 to 19 with a mean value of 5.61 ± 3.12. Pulmonary manifestation including cysts, nodules, and interstitial lung disease were found in 10 patients, eight of whom demonstrated mild to moderate uptake in the lungs. ^{18}F-FDG PET/CT also revealed other findings including hypermetabolic spleen (n = 8) and bone marrow (n = 23), elevated uptake in salivary glands (n = 8). Four patients also underwent follow-up PET/CT scans after therapy, and three of them displayed decreased metabolism.**

Conclusion **^{18}F-FDG PET/CT is a useful tool in the diagnosis, evaluation, and follow-up of MCD by providing systemic manifestations of lymphadenopathy, pulmonary involvement, and hypermetabolic spleen or bone marrow. Furthermore, the lymphadenopathy in MCD presented a predominantly peripheral distribution, relatively symmetric, moderately hypermetabolic, and not confluent pattern on ^{18}F-FDG PET/CT. *Nucl Med Commun* 42: 833–838**

Nuclear Medicine Communications 2021, **42**:833–838

Keywords: Castleman disease, ^{18}F-FDG PET/CT, lymphadenopathy, multicentric

[a]Department of Nuclear Medicine, State Key Laboratory of Complex Severe and Rare Diseases, Peking Union Medical College Hospital, Chinese Academy of Medical Sciences and Peking Union Medical College and [b]Beijing Key Laboratory of Molecular Targeted Diagnosis and Therapy in Nuclear Medicine, Beijing, China

Correspondence to Fang Li, MD, Department of Nuclear Medicine, Peking Union Medical College Hospital, No. 1 Shuaifuyuan, Wangfujing, Dongcheng District, Beijing 100730, China
Tel: + 86 010 69155502; fax: +86 010 69155502;
e-mail: lifang@pumch.cn.

*Yuanyuan Jiang and Guozhu Hou contributed equally to the writing of this article.

Received 2 January 2021 **Accepted** 9 February 2021

Introduction

Castleman disease, also known as angiofollicular or giant lymph node hyperplasia, is a rare lymphoproliferative disorder that was first described in 1954 [1]. Based on the histologic criteria, Castleman disease is classified into three types: hyaline vascular, plasma cell, and mixed cell type [2]. Additionally, Castleman disease is divided clinically as unicentric or multicentric depending on the distribution of the disease. Patients with unicentric Castleman disease (UCD) usually present with a solitary mass and can be treated surgically with a good prognosis [3]. Multicentric Castleman disease (MCD) has a more aggressive clinical course than UCD [4,5]. Patients with MCD presents with systemic symptoms, including fever, anemia, and multifocal lymphadenopathy [6]. Histologically, most MCD were of plasma cell type. MCD is further subclassified according to the presence/absence of HIV/human herpesvirus 8 (HIV/HHV-8) [7]. Almost half of MCD cases are caused by HHV-8 infection in HIV-positive individuals. While approximately half of the patients with MCD are HIV/HHV-8 negative, and these cases were referred to as idiopathic MCD (iMCD) [8].

^{18}F-fluorodeoxyglucose (FDG) PET/computed tomography (CT) has been widely used in the management of various types of malignancies, infectious and noninfectious inflammatory conditions, and lymphoproliferative syndrome [9–11]. A few studies have indicated a possible value for ^{18}F-FDG PET/CT in MCD [12–14]. However, these studies either were in HIV/HHV-8-associated MCD or focused on the correlation between metabolic characteristics and pathological subtypes. Available data

0143-3636 Copyright © 2021 The Author(s). Published by Wolters Kluwer Health, Inc. DOI: 10.1097/MNM.0000000000001404

Fig. 1

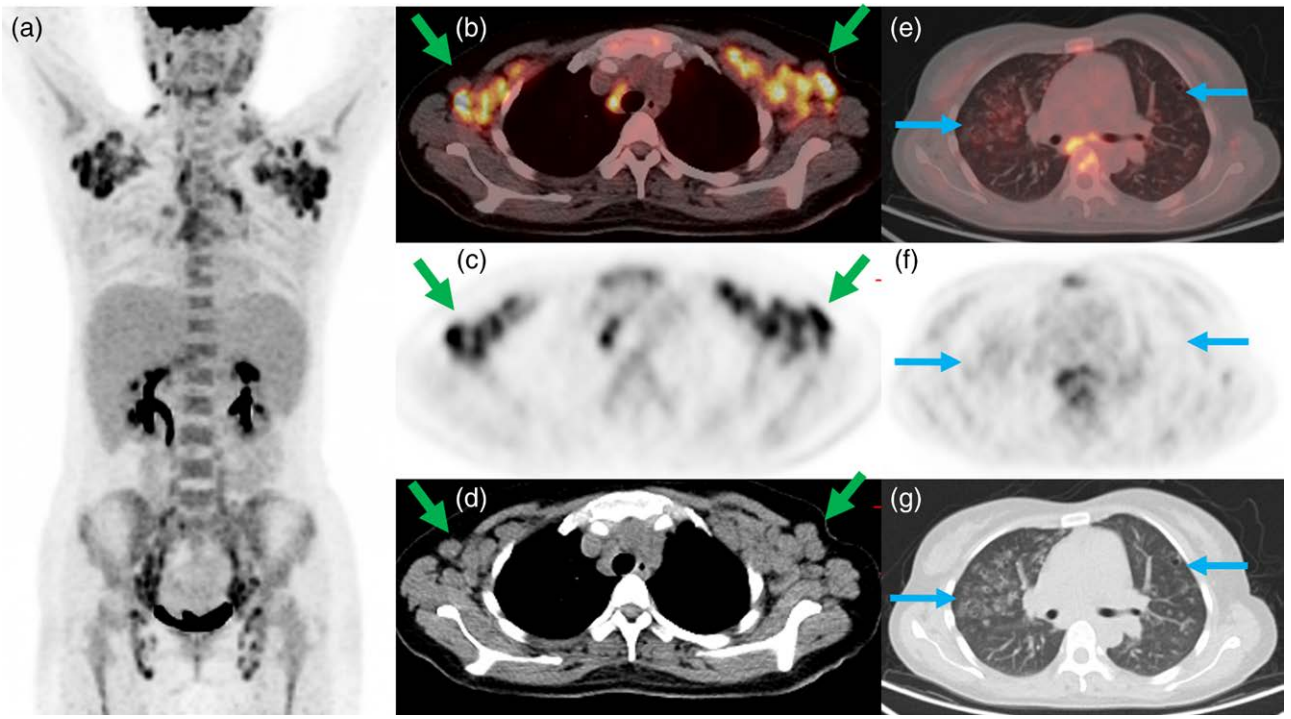

Representative ^{18}F-FDG PET/computed tomography (CT) images of multicentric Castleman disease (MCD) in a 37-year-old woman. The diagnosis of MCD was made by an excisional biopsy of a left cervical lymph node. The PET/CT images demonstrated diffuse hypermetabolic lymphadenopathy in the cervical, axillary, mediastinal, hilar, iliac, and inguinal regions. Note that the most marked lymphadenopathy was in the axillary and inguinal regions (a–d; SUVmax, 7.2). Axial PET/CT images of the chest level revealed multiple thick-walled lung cysts with mild uptake (e–g; arrows; SUVmax, 2.1). FDG, fluorodeoxyglucose.

concerning the ^{18}F-FDG PET/CT findings of iMCD is limited. Therefore, we performed a retrospective study to investigate the role of ^{18}F-FDG PET/CT in characterizing MCD, mainly iMCD.

Methods

Patients

We retrospectively reviewed 35 patients (26 men and nine women; mean age: 43.1 ± 15.5 years) with MCD who underwent ^{18}F-FDG PET/CT between July 2012 and July 2020 in our hospital. MCD diagnosis was made based on the pathological results of lymph node biopsy (n = 32) and lung biopsy (n = 3). Clinical information and laboratory test results were obtained via reviewing the medical records. The pathologic subtype of MCD was determined by reviewing the pathologic reports. In pathological classification, 24 patients were plasma cell type, eight were hyaline vascular type and three were the mixed type. Of all patients, 22 were diagnosed as iMCD, while it remains unknown for the remaining 13 patients, whose data were not documented, whether they were associated with HIV/HHV-8 infection. All patients underwent ^{18}F-FDG PET/CT scans at the initial MCD diagnosis. Four patients additionally underwent ^{18}F-FDG PET/CT scans after treatment. This retrospective study was approved by the institutional review board, and the need for informed consent from subjects was waived because of the retrospective design of the study.

^{18}F-FDG PET/CT study

Following more than 4 h of fasting and ensuring that the blood glucose level was less than 120 mg/dl, all patients received an intravenous administration of ^{18}F-FDG (5.5 MBq/kg). PET/CT scans were started 60 min after injection using a combined PET/CT biograph (Siemens Company, Germany). All scans were performed in a three-dimensional model. A low-dose CT scan was obtained first for attenuation correction and anatomical correlation. Then, emission data were acquired from the skull base to the upper thigh for 2 min per bed.

Image analysis

All the images were retrospectively read by two experienced nuclear medicine physicians. The lymphadenopathy was determined when enlarged and/or hypermetabolic lymph nodes were present. For each scan, 14 lymph node regions were examined: left and right cervical (neck level and supraclavicular/subclavicular fossa), left and right axillary, paravertebral, mediastinal, left and right hilar, abdominal, paraaortic, left and right iliac, and left and right

Fig. 2

Representative [18]F-FDG PET/computed tomography (CT) images of multicentric Castleman disease (MCD) in a 28-year-old man showed diffuse thin-walled cysts in the lungs without increased FDG uptake (a–c). FDG, fluorodeoxyglucose.

inguinal lymph nodes. The CT images were evaluated for the presence of enlarged lymph nodes (short diameter ≥ 1 cm), splenomegaly (craniocaudal size ≥ 13 cm), and pulmonary changes. Hypermetabolic lymph nodes were defined as FDG activity higher than that of adjacent normal soft-tissue structures. Hypermetabolism of the bone marrow and spleen was defined as uptake greater than that of mediastinum and liver, respectively. The maximum standardized uptake value (SUVmax) of each lesion was measured. For lymphadenopathy, the 'highest SUVmax' of any nodal region per patient was determined. The SUVmax from each nodal region was used to determine the median SUVmax of each patient's nodal sites, referred to as 'nodal composite SUVmax'.

Statistical analysis

Descriptive statistics were analyzed using SPSS (IBM SPSS Statistics for Windows, Version 21.0. Armonk, NY), including median, mean value, and SD. Continuous variables were expressed as mean ± SD, while categorical variables were described in numbers and percentages.

Results

[18]F-FDG PET/CT findings

Lymph node findings

Thirty-four out of 35 patients (97.1%) showed increased FDG uptake in at least two nodal regions per patient with a median of nine regions (range: 2–13 regions) (Fig. 1). In all, 13 of 34 patients had ≤5 nodal regions involved; 10 patients had more than five and less than 10 nodal regions involved; and 11 patients had ≥10 regions. The most frequently involved nodal sites were the cervical (n = 31/34; 91.1%), iliac (n = 25; 73.5%), axillary (n = 21; 61.7%), and inguinal (n = 20; 58.8%) areas, and the least common were paraaortic (n = 11; 32.3%) and abdominal (n = 7; 20.5%) nodes (Fig. 1).

None of the 35 patients with lymphadenopathy showed confluent lymph nodes. The largest short-axis diameter of any nodal region in each patient ranged from 0.6 to 2.4 cm (median: 1.2 cm; mean: 1.35 ± 0.43 cm). The highest SUVmax of any nodal region per patient ranged from 2 to 19 with a median value of 4.8 (mean: 5.61 ± 3.12). Only two patients had the 'highest SUVmax' of more than 10 (11.9 and 19, respectively). The 'nodal composite SUVmax' in each patient ranged from 2 to 6.8 with a median value of 3.6 (mean: 3.73 ± 1.16).

Pulmonary involvement

Ten of the present series had pulmonary MCD involvement (Figs. 1 and 2). At CT scans, four patients showed an isolated cystic pattern, three a nodulocystic pattern, one an isolated nodular pattern, and two patients diffuse interstitial pneumonitis pattern with subpleural nodules, centrilobular nodules, interlobular septal thickening, peribronchovascular thickening. Among patients with pulmonary manifestations, eight had mild to moderate FDG uptake in the lungs. The SUVmax ranged from 1.4 to 7.4 (median: 2.4; mean: 2.96 ± 1.90).

Spleen and bone marrow findings

Fifteen patients showed slight or moderate enlargement of the spleen. And eight of them had increased spleen metabolism. The SUVmax of the spleen ranged from 1.8 to 7.1 (median: 3.1; mean: 3.25 ± 1.66). Hypermetabolism in bone marrow was present in 23 patients. The bone marrow SUVmax ranged from 2.5 to 5.7 (median: 3.7; mean: 3.83 ± 0.86). The hypermetabolic bone marrow demonstrated a homogeneous distribution pattern, and no focal abnormal activity was noted.

Salivary gland

Eight patients showed a symmetric increase in salivary gland metabolism (Fig. 3). Of these eight patients, one had increased uptake in the parotid glands; three had increased uptake in the submandibular glands, and four patients presented both parotid and submandibular glands hypermetabolism. The SUVmax of hypermetabolic parotid glands ranged from 2.4 to 3.3 (median: 3.0; mean: 2.92 ± 0.32), while that of submandibular glands ranged from 2.6 to 5.8 (median: 3.5; mean: 3.84 ± 1.15).

Fig. 3

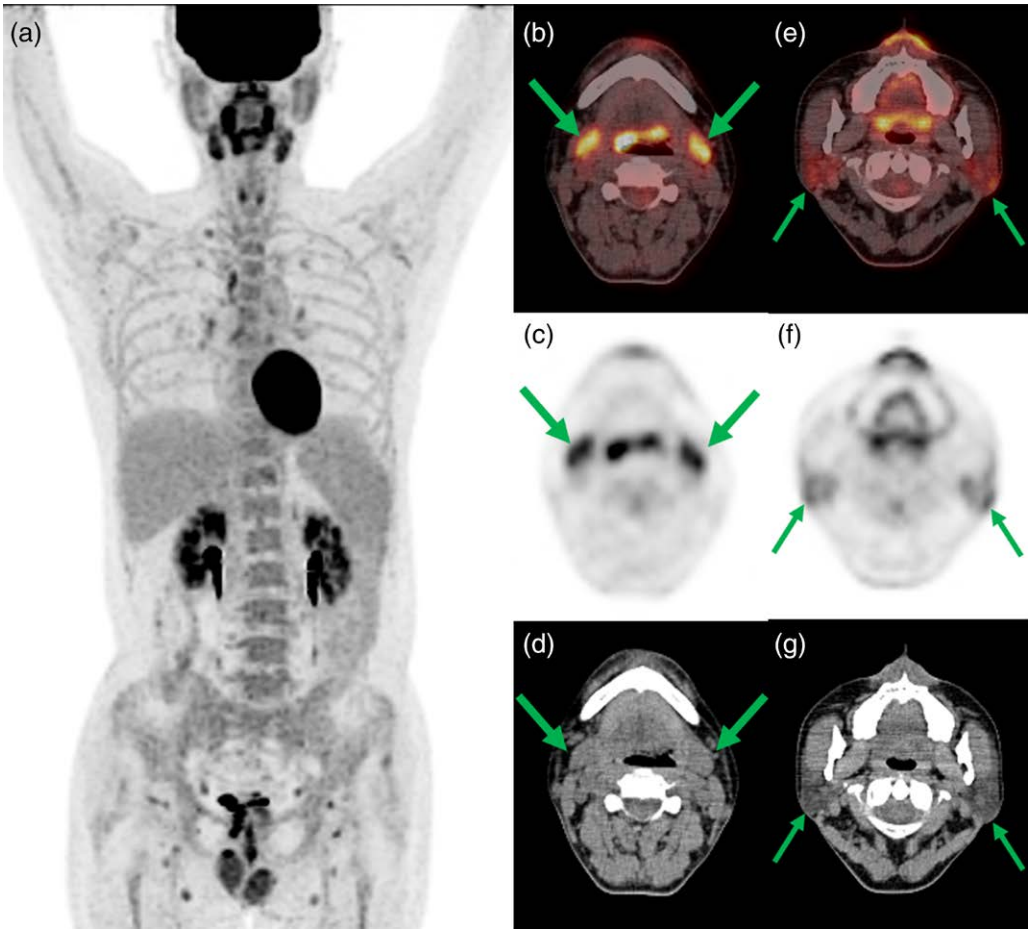

Representative ^{18}F-FDG PET/computed tomography (CT) images of multicentric Castleman disease (MCD) in a 46-year-old man. PET/CT images showed hypermetabolism in bilateral submandibular and parotid glands (a–g, SUVmax, 5.8 and 3.0, respectively). In addition, multiple lymphadenopathies, and moderately hypermetabolic bone marrow and spleen were also noted on PET/CT images. FDG, fluorodeoxyglucose.

Others

In three patients, pleural and abdominopelvic effusions were noted. None of the effusions were FDG avid. In one patient, besides multiple lymphadenopathies, ^{18}F-FDG PET/CT images also showed thickened skin in the buttock region with increased activity (SUVmax: 10.9). Biopsy of the skin revealed infection.

Follow-up images

Follow-up ^{18}F-FDG PET/CT images were available in four of the 35 patients (Fig. 4). The follow-up duration was from 6 to 36 months. All four patients were treated with chemotherapy. Three patients showed a significant decrease in both metabolism and size of the lymphadenopathies. While the remaining one patient had no apparent changes on follow-up scans.

Discussion

The most common presentation of MCD is lymphadenopathy. The previous study has concluded that ^{18}F-FDG PET/CT is effective in evaluating the involved lymph nodes throughout the body in patients with MCD [12,15,16]. In the present study, 97.1% (34/35) patients were found with lymph node involvement with ^{18}F-FDG PET/CT. As demonstrated by our results, the most frequently affected lymph nodes were those located in the cervical, iliac, axillary, and inguinal regions. On the contrary, the least affected were those in the abdominal and paraaortic areas. This finding indicated that the lymphadenopathy of MCD showed a predilection for peripheral over visceral nodal regions. The finding of peripheral distribution of lymphadenopathy in MCD was not pointed out in the previous reports. While we found that lymphadenopathy in the cervical and axillary regions was the most predominant when reviewing the previously published cases with MCD [17] it is unclear why the lymphadenopathy of MCD occurs more frequently in peripheral than visceral nodal regions. We suspected this might be associated with the benign nature of MCD as visceral (mesenteric or paraaortic) lymphadenopathy is more frequently associated with malignant disease.

Fig. 4

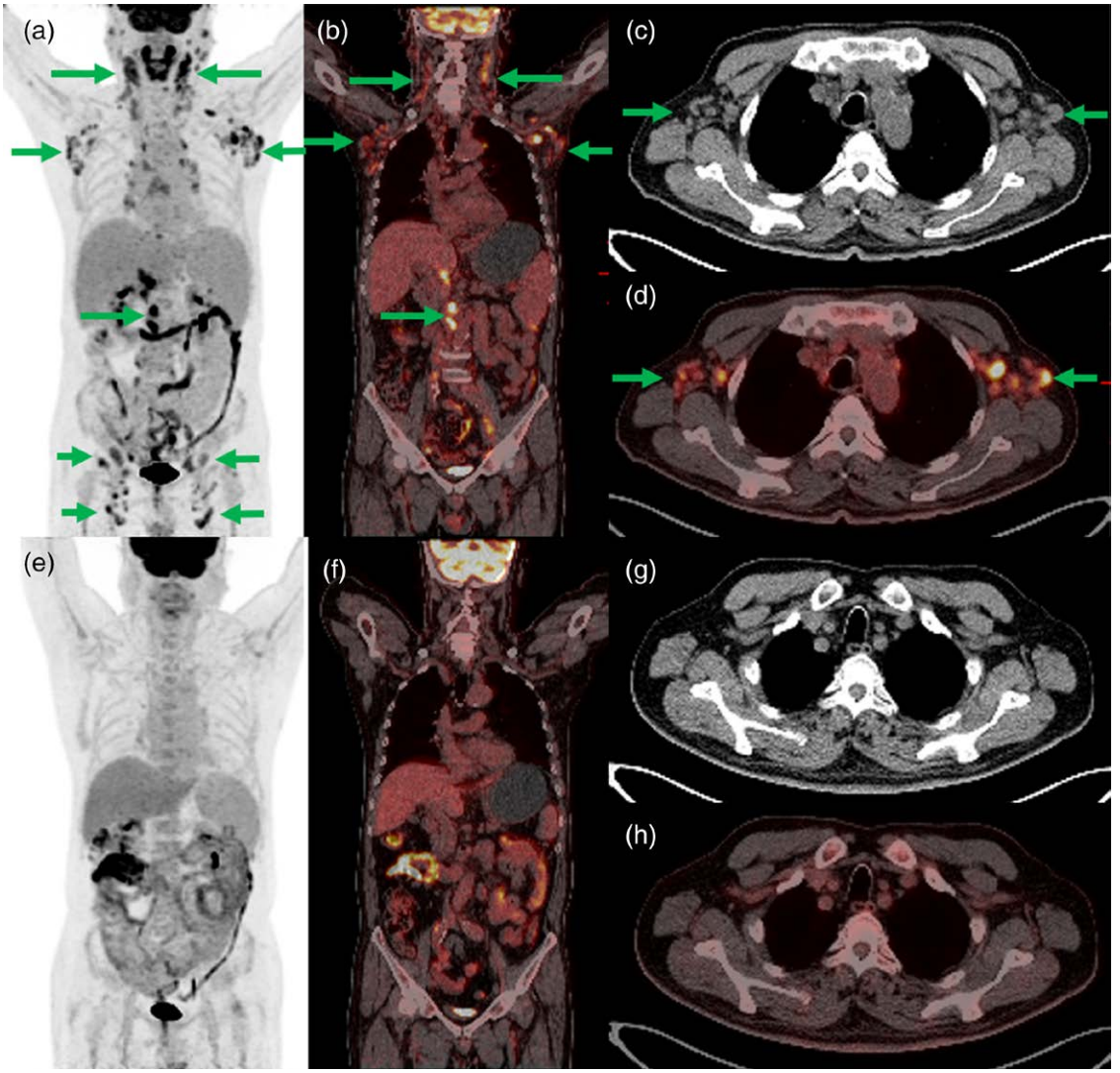

Representative [18]F-FDG PET/computed tomography (CT) images during multicentric Castleman disease (MCD) activity and remission in a 66-year-old man. Pretreatment PET/CT images (a–d) displayed diffuse hypermetabolic lymphadenopathy, splenomegaly with increased metabolism, increased bone marrow metabolism. These abnormalities were observed to have resolved at the remission scans (e–h). FDG, fluorodeoxyglucose.

By visually analyzing the [18]F-FDG PET/CT images, we observed a relatively symmetric distribution of lymphadenopathy. A similar symmetric pattern was also reported in HIV-associated MCD and reactive lymphadenopathy in HIV-infected patients [13,18]. Another feature was that the affected lymph nodes in patients with MCD were not confluent. This can also be reflected by the relatively small size of the lymph nodes. In the research of Hill *et al.*, one patient presented with nonconfluent mesenteric lymphadenopathy at the time of Castleman disease diagnosis but developed into lymphoma with large, confluent mesenteric lymph nodes 9 months later [19]. Although Castleman disease is a benign disease, MCD has the potential for progression to lymphoma. When confluent or large lymph nodes were present, especially in the mesenteric or paraaortic regions, the possibility of transforming to lymphoma should be kept in mind and a biopsy of the hypermetabolic node might be required.

Regarding the metabolic status of the involved lymph nodes, most of the patients in our population demonstrated a moderate FDG uptake with a mean 'highest SUVmax' value of 5.61 ± 3.12, which was in line with the findings from research by Lee *et al.* [14]. They also reported moderately increased FDG uptake in MCD with an average SUVmax of 7.0 ± 4.6. High SUVmax value is uncommon in MCD, and alternative diagnosis (e.g., lymphoma) should be suspected in such cases. In the present patient series, only two patients exhibited the highest SUVmax of more than 10. During the

follow-up, neither of the patients developed lymphoma or other malignancy.

MCD-associated parenchymal lung disease is a less common manifestation of MCD. CT findings of lung cysts, nodules, thickening of bronchovascular bundles, and interlobular septal thickening have been well described in the study by Johkoh *et al*. [20]. And biopsy specimen findings in their study showed that the nodules and interlobular septal thickening at CT scans were the results of the infiltration of lymphocytes and plasma cells. According to our results, six out of 10 patients (60%) were found with multiple cystic changes in the lung, which is slightly lower than the reported 83% (10 out of 12) by Johkoh *et al*. [20], probably due to the small number of patients with pulmonary involvement in our population. In this study, some of the thick-wall cysts were observed to have mild to moderate FDG uptake in the cyst wall. We suspected that the FDG activity in the cyst wall might be related to the infiltration of lymphocytes and plasma cells.

Some of the patients in this study also presented with hypermetabolic spleen or bone marrow on ^{18}F-FDG PET/CT scans, which are probably due to the reactive changes of an activated hematological system. These findings were not specific, as they can also be seen in other hematological, immunological, and inflammatory diseases.

This study has several limitations, which are mainly due to its retrospective design and small sample size. Most of the patients in our population did not undertake follow-up PET/CT scans, precluding comprehensive assessment of the role of ^{18}F-FDG PET/CT in monitoring treatment response. Regarding pulmonary involvement, pathological examinations of lung lesions were performed in only two patients; therefore, we could not perform a detailed radiopathologic investigation.

Conclusion

In summary, ^{18}F-FDG PET/CT is a useful tool in the diagnosis, evaluation, and follow-up of MCD by providing systemic manifestations of lymphadenopathy, pulmonary involvement, and hypermetabolic spleen or bone marrow. Furthermore, the lymphadenopathy in MCD presented a predominantly peripheral distribution, relatively symmetric, moderately hypermetabolic, and not confluent pattern on ^{18}F-FDG PET/CT in this study.

Acknowledgements

Conception and design were done by Wuying Cheng and Fang Li. Financial support by Wuying Cheng and Fang Li. Collection and assembly of data were done by Yuanyuan Jiang, Guozhu Hou, Zhaohui Zhu, and Li Huo. Writing was done by Yuanyuan Jiang and Guozhu Hou.

This study was supported by the National Key Research and Development Program of China (2016YFC0901500).

Conflicts of interest

There are no conflicts of interest.

References

1 Castleman B, Towne VW. Case records of the Massachusetts general hospital: case no. 40231. *N Engl J Med* 1954; **250**:1001–1005.
2 Keller AR, Hochholzer L, Castleman B. Hyaline-vascular and plasma-cell types of giant lymph node hyperplasia of the mediastinum and other locations. *Cancer* 1972; **29**:670–683.
3 Shin DY, Jeon YK, Hong YS, Kim TM, Lee SH, Kim DW, *et al*. Clinical dissection of multicentric Castleman disease. *Leuk Lymphoma* 2011; **52**:1517–1522.
4 Kligerman SJ, Auerbach A, Franks TJ, Galvin JR. Castleman disease of the thorax: clinical, radiologic, and pathologic correlation: from the radiologic pathology archives. *Radiographics* 2016; **36**:1309–1332.
5 Enomoto K, Nakamichi I, Hamada K, Inoue A, Higuchi I, Sekimoto M, *et al*. Unicentric and multicentric Castleman's disease. *Br J Radiol* 2007; **80**:e24–e26.
6 Herrada J, Cabanillas F, Rice L, Manning J, Pugh W. The clinical behavior of localized and multicentric Castleman disease. *Ann Intern Med* 1998; **128**:657–662.
7 Fajgenbaum DC, Uldrick TS, Bagg A, Frank D, Wu D, Srkalovic G, *et al*. International, evidence-based consensus diagnostic criteria for HHV-8-negative/idiopathic multicentric Castleman disease. *Blood* 2017; **129**:1646–1657.
8 Dispenzieri A, Fajgenbaum DC. Overview of Castleman disease. *Blood* 2020; **135**:1353–1364.
9 Haroon A, Zumla A, Bomanji J. Role of fluorine 18 fluorodeoxyglucose positron emission tomography-computed tomography in focal and generalized infectious and inflammatory disorders. *Clin Infect Dis* 2012; **54**:1333–1341.
10 Carrasquillo JA, Chen CC, Price S, Whatley M, Avila NA, Pittaluga S, *et al*. 18F-FDG PET imaging features of patients with autoimmune lymphoproliferative syndrome. *Clin Nucl Med* 2019; **44**:949–955.
11 Gallicchio R, Mansueto G, Simeon V, Nardelli A, Guariglia R, Capacchione D, *et al*. F-18 FDG PET/CT quantization parameters as predictors of outcome in patients with diffuse large B-cell lymphoma. *Eur J Haematol* 2014; **92**:382–389.
12 Barker R, Kazmi F, Stebbing J, Ngan S, Chinn R, Nelson M, *et al*. FDG-PET/CT imaging in the management of HIV-associated multicentric Castleman's disease. *Eur J Nucl Med Mol Imaging* 2009; **36**:648–652.
13 Polizzotto MN, Millo C, Uldrick TS, Aleman K, Whatley M, Wyvill KM, *et al*. 18F-fluorodeoxyglucose positron emission tomography in kaposi sarcoma herpesvirus-associated multicentric Castleman disease: correlation with activity, severity, inflammatory and virologic parameters. *J Infect Dis* 2015; **212**:1250–1260.
14 Lee ES, Paeng JC, Park CM, Chang W, Lee WW, Kang KW, *et al*. Metabolic characteristics of Castleman disease on 18F-FDG PET in relation to clinical implication. *Clin Nucl Med* 2013; **38**:339–342.
15 Ma Y, Li F, Chen L. Widespread hypermetabolic lesions due to multicentric form of Castleman disease as the cause of fever of unknown origin revealed by FDG PET/CT. *Clin Nucl Med* 2013; **38**:835–837.
16 Ding Q, Zhang J, Yang L. (18)F-FDG PET/CT in multicentric Castleman disease: a case report. *Ann Transl Med* 2016; **4**:58.
17 Guazzaroni M, Bocchinfuso F, Vasili E, Lacchè A, Ranalli T, Garipoli A, *et al*. Multicentric Castleman's disease: report of three cases. *Radiol Case Rep* 2019; **14**:328–332.
18 Mhlanga JC, Durand D, Tsai HL, Durand CM, Leal JP, Wang H, *et al*. Differentiation of HIV-associated lymphoma from HIV-associated reactive adenopathy using quantitative FDG PET and symmetry. *Eur J Nucl Med Mol Imaging* 2014; **41**:596–604.
19 Hill AJ, Tirumani SH, Rosenthal MH, Shinagare AB, Carrasco RD, Munshi NC, *et al*. Multimodality imaging and clinical features in Castleman disease: single institute experience in 30 patients. *Br J Radiol* 2015; **88**:20140670.
20 Johkoh T, Müller NL, Ichikado K, Nishimoto N, Yoshizaki K, Honda O, *et al*. Intrathoracic multicentric Castleman disease: CT findings in 12 patients. *Radiology* 1998; **209**:477–481.